Journal of Solid State Chemistry 183 (2010) 1841–1846

Contents lists available at ScienceDirect

Journal of Solid State Chemistry

journal homepage: www.elsevier.com/locate/jssc

Two 3D networks based on sandwich-type polyoxometalate units linked by Sr–O clusters: Synthesis, structure, and magnetic property

Yang Yu [a,c], Bai-Bin Zhou [a,b,*], Kai Yu [a,b], Yu-Nan Zhang [b]

[a] Key Laboratory of Materials Physics and Chemistry, Colleges of Heilongjiang Province, Harbin Normal University, Harbin 150080, PR China
[b] Department of Applied Chemistry, Harbin Institute of Technology, Harbin 150001, PR China
[c] Heilongjiang Beikai Professional and Technology College, Harbin 150317, PR China

ARTICLE INFO

Article history:
Received 23 April 2010
Received in revised form
5 June 2010
Accepted 8 June 2010
Available online 15 June 2010

Keywords:
Polyoxometalates
Sandwich complexes
Strontium
High-coordinated
Magnetic property

ABSTRACT

Two 3D hybrid sandwich-type polyoxometalates, $[\{Sr(H_2O)_5Sr(H_2O)_6Sr_{0.5}(H_2O)_7\}_2Mn_4(H_2O)_2(\alpha\text{-}PW_9O_{34})_2]\cdot 6H_2O$ (**1**) and $[\{Sr(H_2O)_6[Sr(H_2O)_8]_2Sr(H_2O)_4\}_2Mn_4(H_2O)_2(\alpha\beta\beta\alpha\text{-}P_2W_{15}O_{56})_2]\cdot 5H_2O$ (**2**), have been obtained by the routine synthetic reactions in aqueous solution and characterized by IR, elemental analysis, thermal analysis, and X-ray single-crystal diffraction. The 3D hybrid framework of **1** and **2** are built by tetra-Mn^{II} substituted sandwich-type polyoxotungstates modified by fourteen $Sr(H_2O)_x$ (x=4–8) units acting as bridges, forming centrosymmetric sandwich structures. The magnetic property of compound **1** has been studied by measuring its magnetic susceptibility in the temperature range of 2–300 K, which indicates predominant ferromagnetic interactions between the Mn^{II}–O–Mn^{II} bridge unit. Additionally, the electrochemical behaviours have been detected on solid bulk modified carbon paste electrodes of compounds (CPEs) and three redox couples are detected.

1. Introduction

Transition-metal-polyoxometalates (TMSPs) based on lacunary Keggin and Wells–Dawson polyanions precursors exhibit a fascinating variety of structures and properties including catalysis, medicine, and magnetism [1]. The lacunary polyanions, such as monovacant, divacant, trivacant, were important intermediates in POM chemistry and were proved to be metal-accommodated species that can combine with TMs or rare earths including Mn, Cu, Co, Ni, Zn, Zr, Hf, Ce, and so on [2], making the structure stable and polymerization clusters via extremely strong connection. The vacant sites in the surface of POMs can provide more O-donor ligands and more negative charges, which have been proved as the most active sites to react with various metal ions or metal-organic fragments. In the context, trivacant heteropolytungstates, such as $\alpha\text{-}PW_9O_{34}^{9-}$ or $\alpha\text{-}P_2W_{15}O_{56}^{12-}$, acting as structural building blocks, are of particular interest because the trivacant species are suitable precursors that can react with d-electron metal ions in their three vacant sites to form dimeric sandwich-type structure [3]. Meanwhile, the structural multiplicities could be adjusted by introducing of diverse bridging units and transition metal ions [4]. The trivacant POMs and the paramagnetic TM aggregations could combine to novel high-coordinated and high-connected TMSPs. Up to now, numerous sandwich-type POMs have been synthesized, which belong to the well-known Weakley-, Herve-, Krebs- and Knoth-type sandwich structures as the main building blocks with various nuclearities and original topologies. The Yang's and Hill's group have reported plenty of novel sandwich-type structures based on trivacant Keggin (PW_9, SiW_9, and GeW_9) and Wells–Dawson (P_2W_{15}) POMs, respectively [5].

To the best of our knowledge, the muti-dimentional sandwich trivacant heteropolytungstates structures connecting with each other in different ways via some kind of metal–water units (alkaline metal (K, Na), transition metal (Mn, Co), lanthanum (Ce)) have been reported [6], however, the alkaline-earth metal ions act as linkage to form three dimensional structure are never been reported, except that alkaline-earth metal ions (Sr or Ca) fill in vacant position or cavum [7]. Therefore, it is still meaningful and challenging to synthesize new complexes that alkaline-earth metal ions act as linkages. In our work, we try to find the rational reaction condition to obtain stable sandwich-type heteropolytungstates and the alkaline-earth metal Sr^{II} ion. With the aim of extending these new series to other interesting sandwich complexes, we report the synthesis, crystal structures, and magnetic properties of two compounds consisting of $\alpha\text{-}PW_9O_{34}^{9-}$ or $\alpha\text{-}P_2W_{15}O_{56}^{12-}$, transition metal, and alkaline-earth metal, $[\{Sr(H_2O)_5Sr(H_2O)_6Sr_{0.5}(H_2O)_7\}_2Mn_4(H_2O)_2(\alpha\text{-}PW_9O_{34})_2]\cdot 6H_2O$ (**1**) and $[\{Sr(H_2O)_6[Sr(H_2O)_8]_2Sr(H_2O)_4\}_2Mn_4(H_2O)_2(\alpha\beta\beta\alpha\text{-}P_2W_{15}O_{56})_2]\cdot 5H_2O$ (**2**). The magnetic properties of **1** and the electrochemistry behaviours are studied additionally.

* Corresponding author at: Key Laboratory of Materials Physics and Chemistry, Colleges of Heilongjiang Province, Harbin Normal University, Harbin 150080, PR China.
E-mail address: zhou_bai_bin@163.com (B.-B. Zhou).

0022-4596/$ - see front matter © 2010 Elsevier Inc. All rights reserved.
doi:10.1016/j.jssc.2010.06.005

2. Experimental

2.1. Materials and methods

$K_9[PW_9O_{34}]\cdot nH_2O$ and $K_{12}[P_2W_{15}O_{56}]\cdot nH_2O$ [8] was prepared according to the literature method and confirmed by IR spectroscopy. All of the other chemicals were obtained from commercial sources and used without further purification. P, W, Mn, and Sr were analyzed on a PLASMA-SPEC (I) ICP atomic emission spectrometer. Elemental analyses (C, H, and N) were performed on a Perkin-Elmer 2400 CHN elemental analyzer. The IR spectra were obtained on an Alpha Centauri Fourier transform IR (FT-IR) spectrometer with KBr pellets in the 400–4000 cm^{-1} region. The thermo gravimetric analyses (TGA) were carried out in N_2 on a Perkin-Elmer DTA 1700 differential thermal analyzer with a rate of 10 °C/min. Magnetic susceptibility data were collected over the temperature range of 2–300 K in a magnetic field of 1000 Oe on a Quantum Design MPMS-5 SQUID magnetometer. Electrochemical measurements were performed with a CHI660 electrochemical workstation. A conventional three-electrode system was used. The working electrode was a modified carbon paste electrode (CPE), a platinum wire as the counter electrode and Ag/AgCl (3M KCl) electrode was used as a reference electrode. X-ray powder diffractometry (XRPD) study of **1** was performed with a NETZSCH STA 449C instrument, with a panalytical X-pert pro diffractometer and Cu$K\alpha$ radiation.

2.2. Synthesis of *1* and *2*

Compound **1** was synthesized in aqueous condition. $K_9[PW_9O_{34}]\cdot nH_2O$ (0.5 g) was dissolved in 50 mL water, then $MnCl_2\cdot 2H_2O$ (0.17 g) and $SrCl_2\cdot 6H_2O$ (0.26 g) were added. The solution was heated to 70 °C, the pH value was adjusted to 4.6 with 6 M HCl until the precipitation appearing. After 2 h, the solution was cooled to room temperature and 2 days later, the orange block crystals (0.15 g, yield 48%) were obtained based on W. Anal. Calcd. for $H_{68}Mn_4O_{112}P_2Sr_5W_{18}$ (1) (Mr=5889.5) (%): W, 56.17; Mn, 3.73; P, 1.05; Sr, 7.44. Found (%): W, 56.16; Mn, 3.78; P, 1.02; Sr, 7.40.

The preparation of **2** was similar to that of **1**, except that $K_{12}[P_2W_{15}O_{56}]\cdot nH_2O$ was instead of $K_9[PW_9O_{34}]\cdot nH_2O$. Anal. Calcd. for $H_{86}Mn_4O_{171}P_4Sr_8W_{30}$ (2) (Mr=9382.5) (%): W, 58.77; Mn, 2.34; P, 1.32; Sr, 7.47. Found (%): W, 58.76; Mn, 2.38; P, 1.35; Sr, 7.44.

2.3. X-ray crystallography

The reflection intensities of **1** and **2** were collected on a Bruker SMART CCD diffractometer with Mo$K\alpha$ radiation (λ=0.71703 Å) at 273 K in the range of $2.57^\circ < \theta < 28.28^\circ$. The structure was solved by direct methods with SHELXS-97 and refined by full-matrix least-squares method on F^2 using the SHELXL-97 crystallographic software package [9]. Crystallographic data for the structure of **1** and **2** reported in this paper has been applied CSD numbers 420908 and 421055. Copy of the data can be obtained free of charge from the FIZ Karlsruhe, Eggenstein-Leopoldshafen, Germany (Fax: +49 7247 808 666; E-mail: crysdata@fiz-karlsruhe.de). The crystallographic data and structure determination parameters for **1** and **2** were summarized in Table 1. Selected bond lengths and bond angles are provided in Tables S1 and S2 in the Supporting Information.

Table 1
Crystal data and structural refinement for compounds **1** and **2**.

Compound	**1**	**2**
Empirical formula	$H_{68}Mn_4O_{112}P_2Sr_5W_{18}$	$H_{86}Mn_4O_{171}P_4Sr_8W_{30}$
Formula weight	5889.5	9382.5
Crystal system	Triclinic	Triclinic
space group	$P-1$	$P-1$
Unit-cell dimensions	a=12.1382(4), b=12.7200(5), c=18.2212(9) α=104.0780(10), β=97.9210(10), γ=114.7620(10)	a=14.624(3), b=16.590(3), c=16.628(3) α=89.16(3), β=88.52(3), γ=78.37(3)
Volume	2384.40(17)(Å^3)	3949.8(14)
Z	1	1
ρ_{calc} (g/cm^3)	4.102	3.944
μ (mm^{-1})	25.054	24.886
F(000)	2616.0	4138.0
Crystal size (mm)	0.38 × 0.36 × 0.14	0.18 × 0.15 × 0.12
Goodness-of-fit on F^2	1.042	1.035
Final R indices ($I > 2\sigma(I)$)	R_1=0.0473, wR_2=0.1407	R_1=0.0591, wR_2=0.1413
R indices (all data)	R_1=0.0511, wR_2=0.1442	R_1=0.0805, wR_2=0.1620

3. Results and discussions

3.1. Synthesis

Compounds **1** and **2** were synthesized by treating precursors of $K_9[PW_9O_{34}]\cdot nH_2O$ (for **1**) and $K_{12}[P_2W_{15}O_{56}]\cdot nH_2O$ (for **2**), $MnCl_2\cdot 2H_2O$, and $SrCl_2\cdot 2H_2O$ at 70 °C. The successful syntheses indicate that the $Sr(H_2O)_x$ unit is an effective linker in these reaction system because Sr^{II} ions have multi-coordinated environments. We have studied diverse different reaction environment: (1) change the reaction system into H_3PO_4, Na_2WO_4, $MnCl_2\cdot 2H_2O$, and $SrCl_2\cdot 2H_2O$ according to the P-W ratio of POMs; (2) change the same group $MgCl_2$, $CaCl_2$, $BaCl_2$ instead of $SrCl_2$; (3) adjust the pH value to the lower or the higher level; and (4) utilize the hydrothermal synthesis method maintaining the same reactants. The results are we fail to obtain **1** and **2**. Through the exploring experiments, we can conclude that both type of precursors (POMs and salt), the pH value, synthesis methods are key factors for synthesizing these two complexes.

3.2. Structure descriptions

Single-crystal X-ray diffraction analysis reveals that **1** exhibits a sandwich-type structure constructed from two α-$PW_9O_{34}^{9-}$ units, four Mn^{2+} ions, five $Sr(H_2O)_x$ (x=5, 6, 7) units, and six lattice waters, resulting in a rarely 14-supported structure (Fig. 1a). In the cluster, α-$PW_9O_{34}^{9-}$ units possess the well-known trivacant Keggin structural A-α-type, resulting from the removal of three edge-sharing {WO6} octahedral in the α-Keggin-type structure. All W centers display the octahedral coordination geometry. The W–O bond lengths vary from 1.710(11) to 2.443(11) Å and the O–W–O angles in the range of 72.8(4)–170.0(5)°. The central belt of **1** is composed of a rhombic Mn_4O_{16} group, in which four coplanar MnO_6 octahedra connected with each other in an edge-sharing mode. The bond lengths of Mn–O are in the range of 2.066(10)–2.311(10) Å (Fig. 1b). The distances of Mn···Mn along the sides of the rhombus are 3.37 Å while along the diagonal of the rhombus are 3.35 and 5.80 Å. The crystallographically independent Sr–O clusters have different coordination environments. Sr1 center is coordinated with a terminal oxygen atom derived from $\{PW_9O_{34}\}$ units, two μ–O bridge (O55) from adjacent Sr1 center and six

coordinated water molecules, possessing an eight-coordination environment. Sr2 center exhibits eight-coordination geometry too, formed by three terminal oxygen atoms from three $\{PW_9O_{34}\}$ fragments and five coordinated water molecules. Sr3 center are nine-coordinated and coordinated with three terminal oxygen atoms derived form $\{PW_9O_{34}\}$ fragments and six coordinated water molecules (Fig. 2). In summary, the coordination number and the coordination modes of Sr^{2+} ions together lead to the formation of high-connected 3D structure, which testifies to our synthetic strategy. The lengths of Sr–O are in the range of 2.530(14)–2.830(11) Å, and the angles of O–Sr–O are in the range of 36.7(3)–144.9(3)°. Bond valence sum calculations indicate that the oxidation states of all W, Mn, Sr centers exhibit +6, +2, +2, respectively.

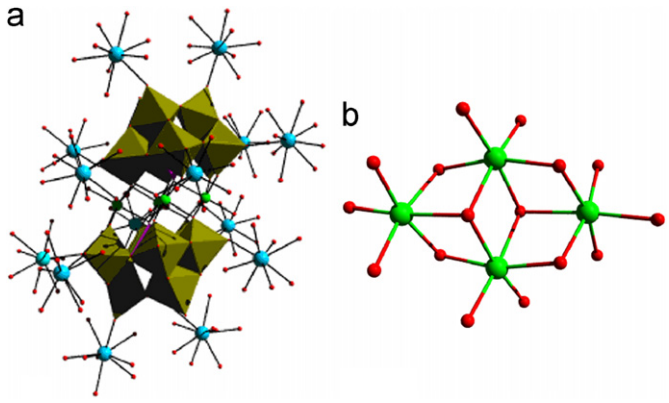

Fig. 1. (a) Polyhedral plot showing the structure of compound **1**. Hydrogen atoms, solvent water molecules are omitted for clarity and (b) ball-and-stick representation of central belt in **1**.

It is very interesting that compound **1** are modified by 14 Sr–O clusters, which could be viewed as μ_2-bridges to connect with adjacent sandwich-type polyanions, to form 3D open-framework rationalized as a (3, 3, 14) network, with the topology symbol $\{4^{20}\cdot6^{28}\cdot8^{18}\}\{4^3\}_4$ (Fig. 3a and b), when $[Mn_4(H_2O)_2(\alpha\text{-}PW_9O_{34})_2]^{10-}$ clusters are taken as 14-connected nodes, Sr2 and Sr3 atoms are seemed as three-connected nodes. Additionally, the coordination geometry of a $[Mn_4P_2W_{18}]$ fragment is shown in Fig. 3c.

Compound **2** is composed of a 14-supporting sandwich-type polyanion $[Mn_4(H_2O)_2(\alpha\beta\beta\alpha\text{-}P_2W_{15}O_{56})_2]^{16-}$, eight $Sr(H_2O)_x$ (x=4, 6, 8) groups, and five lattice water molecules (Fig. 4). It is well known that the reaction of the $[P_2W_{15}O_{56}]^{12-}$ unit with transition-metal cations yields sandwich complexes, in which a sheet of four Mn atoms (two internal and two external, Fig. 1a) is sandwiched between two $[P_2W_{15}O_{56}]^{12-}$ subunits. For **2**, tetranuclear sandwich complexes, the 'classical' ββ configuration is observed with β connectivity between both trivacant $[P_2W_{15}]$ units and the central Mn_4 tetrad. This type of arrangement leads to a molecular anion with C_{2h} symmetry in which the two $[P_2W_{15}]$ moieties are equivalent [10].

The well-known sandwich-type polyoxoanion consists of two trivacant $[\alpha\beta\beta\alpha\text{-}P_2W_{15}O_{56}]^{12-}$ Dawson moieties sandwiching a central symmetric rhomb-like $Mn_4(H_2O)_2$ segment via the W–O–Mn and P–O–Mn connecting modes. All the W and Mn centers exhibit the octahedral coordination environments. The bond lengths of W–O are in the range of 1.64(4)–2.42(3) Å, while the bond lengths of Mn–O are in the range of 2.11(3)–2.37(9) Å. The $Sr(H_2O)_x$ groups have different coordination environments (Fig. 5). The lengths of Sr–O are in the range of 1.62(4)–2.812(10) Å, and the angles of O–Sr–O are in the range of

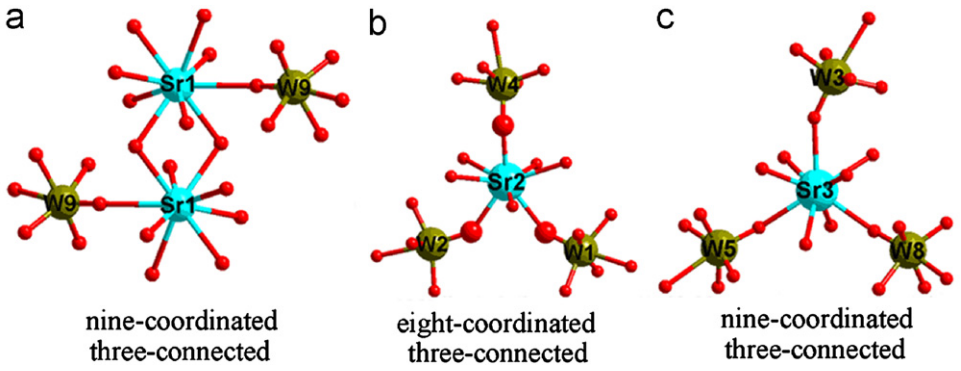

Fig. 2. Coordination environments of Sr1, Sr2, Sr3 of **1**.

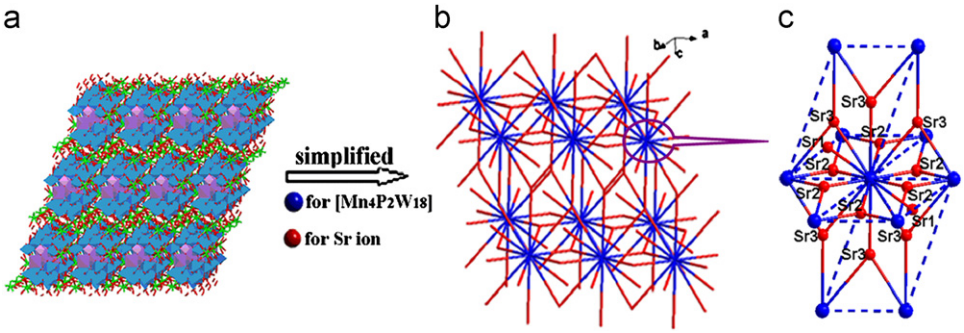

Fig. 3. (a) Polyhedral/stick representation of the 3D structure of **1**. (b) View of the topology of compound **1** (the blue nodes symbolize the $[Mn_4(H_2O)_2(\alpha\text{-}PW_9O_{34})_2]^{10-}$ clusters, and the red nodes symbolize Sr atoms). (c) The coordination environments of a $[Mn_4(H_2O)_2(\alpha\text{-}PW_9O_{34})_2]^{10-}$ fragment. (For interpretation of the references to colour in this figure legend, the reader is referred to the web version of this article.)

48.5(19)–172.5(17)°. Similarly, compound **2** also exhibits 3D framework via $Sr(H_2O)_x$ groups and POMs. Furthermore, the 3D structure is a connecting network with $\{4^3\}_2\{4^8\cdot6^6\cdot8^{27}\cdot12^4\}\{4\}_2$ topology(Fig. 6a and b), if we assign $[Mn_4(H_2O)_2(\alpha\beta\beta\alpha\text{-}P_2W_{15}O_{56})_2]^{16-}$ units and effectively connected Sr atoms as nodes. In this simplification, $[Mn_4(H_2O)_2(\alpha\beta\beta\alpha\text{-}P_2W_{15}O_{56})_2]^{16-}$ clusters are taken as 10-connected nodes while Sr atoms are two/three-connected nodes. The coordination geometry of a $[Mn_4(H_2O)_2(\alpha\beta\beta\alpha\text{-}P_2W_{15}O_{56})_2]^{16-}$ polyanion fragment is shown in Fig. 6c.

Compared with **1** and **2**, there are three noticeable features. First, the $\{PW_9O_{34}\}$ and $[P_2W_{15}]$ clusters act as muti-dentate inorganic ligand coordinating to 14 Sr units. They both represent the high connection number. The difference is that when form 3D structures, $\{PW_9O_{34}\}$ is taken as 14-connected nodes, while $[Mn_4P_4W_{30}]$ clusters are taken as 10-connected nodes. Second, the POMs exhibit various coordination fashions, including the polar position and the equator positions. Finally, Sr atoms also represent multiple coordination geometries in **1** and **2**. There are three crystallographically independent Sr atoms (Sr1, Sr2, and Sr3) for **1** and four for **2**, which exhibit various sorts of coordination geometries coexisting in the structure. In compounds **1** and **2**, the adjacent polyanions together with Sr–O linkages constituted 1D chains along *a*-, *b*-, *c*-axis and 2D layers on *ab*-, *ac*-, *bc*-plane (Schemes S1 and S2).

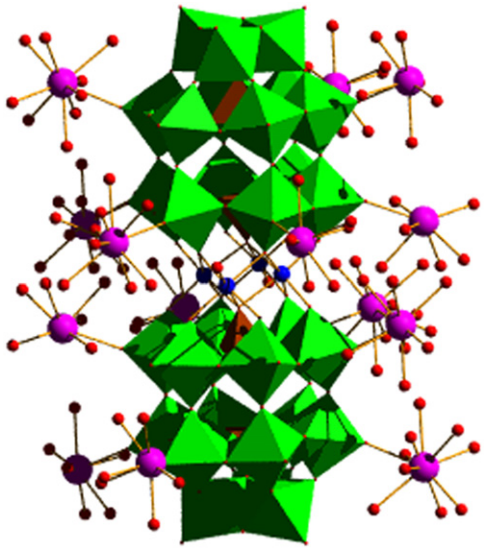

Fig. 4. Polyhedral plot showing the structure of compound **2**. Hydrogen atoms, solvent water molecules are omitted for clarity.

3.3. Spectroscopic and thermal analysis

For explaining the structure additionally, we test the IR of the two complexes. The IR spectra of compounds **1** and **2** recorded between 400 and 4000 cm^{-1} with KBr pellet (Fig. S1) are similar: the characteristic peaks at 1030, 1090 attribute to $\nu(P\text{–}O_a)$, the features at 937, 876, 753, and 508 cm^{-1} for **1**, 931, 765, and 520 cm^{-1} for **2** can be ascribed to $\nu(W\text{–}O_t)$, $\nu(W\text{–}O_b\text{–}W)$, and $\nu(W\text{–}O_c\text{–}W)$ (where O_t=terminal oxygen, O_b=bridged oxygen of two octahedral sharing a corner, and O_c=bridged oxygen of two octahedral sharing an edge). And 3416 and 3428 cm^{-1} regions are indicative of $\nu(O\text{–}H)$. The results are consistent with the feature of the structures.

The X-ray diffraction confirms that **1** and **2** contain amount of coordinated water and lattice water molecules, so the TG analysis is indispensable. The thermal stabilities of compounds **1** and **2** were investigated under a N_2 atmosphere from 30 to 800 °C, and the TG curves are shown in Fig. S2. The TG curve of **1** and **2** gives a total weight loss of 13.37 (calcd. 13.45%) and 11.42 (calcd. 11.32%) in the range of 50–700 °C, corresponding to the loss of all coordinated water and lattice water molecules. All the weight loss from the TG curves accord with the formulas of compounds **1** and **2**.

3.4. Electrochemical behavior

In spite of **1** and **2** are soluble in water, it is not certain that the entire coordination networks of **1** and **2** remains intact in solution. The CPEs become optimal choices to study the electrochemical properties and are measured in the potential range from 800 to −600 [11]. The experiments are carried out in 1 M H_2SO_4 aqueous solution. Cyclic voltammograms of **1**-CPE and **2**-CPE are shown in Fig. 7, three pairs of reversible redox peaks (I–I′, II–II′, and III–III′) appeared, and the mean peak potentials $E_{1/2}=(E_{pc}+E_{pa})/2$ were −352, −103, and 479 mV (compound **1**), −340, −106, and 483 mV (compound **2**), respectively, corresponding to two-electron redox processes of W^{6+}/W^{5+} [12]. With the scan rates increasing, the peak currents are proportional to the scan rates and the increase extent of the anodic and cathodic peak currents are almost the same. The peak potentials changed gradually: the cathodic peak potentials shifted to the negative direction and the corresponding anodic peak potentials to the positive direction, namely, the peak-to-peak separation between the corresponding cathodic and anodic peaks increased. The results verify that the redox ability of the trivacant hydropolyanions of **1** and **2** can be maintained in the solids, which promises a potential application of this kind of inorganic framework materials in electrochemistry. The W-system is found to be well-separated to each other, promoting the sequential study in electrochemistry.

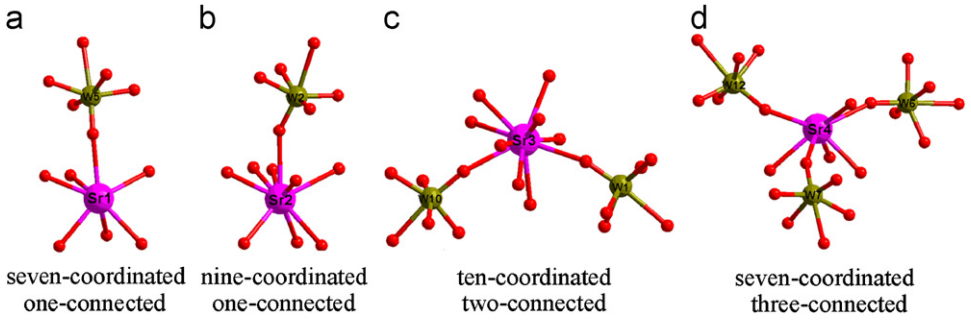

Fig. 5. Coordination environments of Sr1, Sr2, Sr3, Sr4 of **2**.

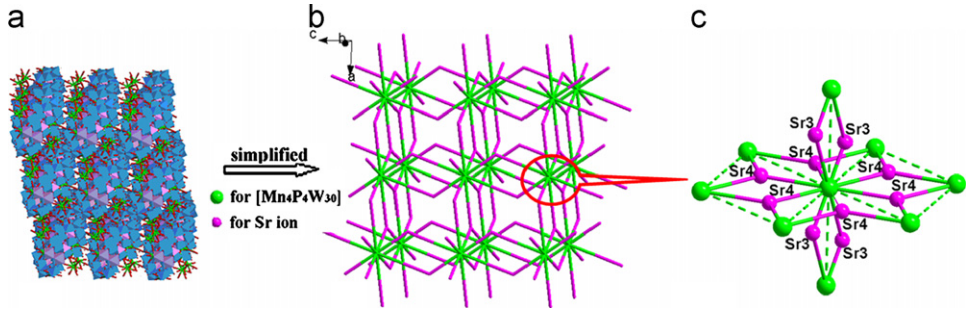

Fig. 6. (a) Polyhedral/stick representation of the 3D structure of **2**, (b) view of the topology of compound **2** (the green nodes symbolize the $[Mn_4(H_2O)_2(\alpha\beta\beta\alpha\text{-}P_2W_{15}O_{56})_2]^{16-}$ clusters, and the pink nodes symbolize Sr atoms), and (c) the coordination environments of a $[Mn_4(H_2O)_2(\alpha\beta\beta\alpha\text{-}P_2W_{15}O_{56})_2]^{16-}$ fragment. (For interpretation of the references to colour in this figure legend, the reader is referred to the web version of this article.)

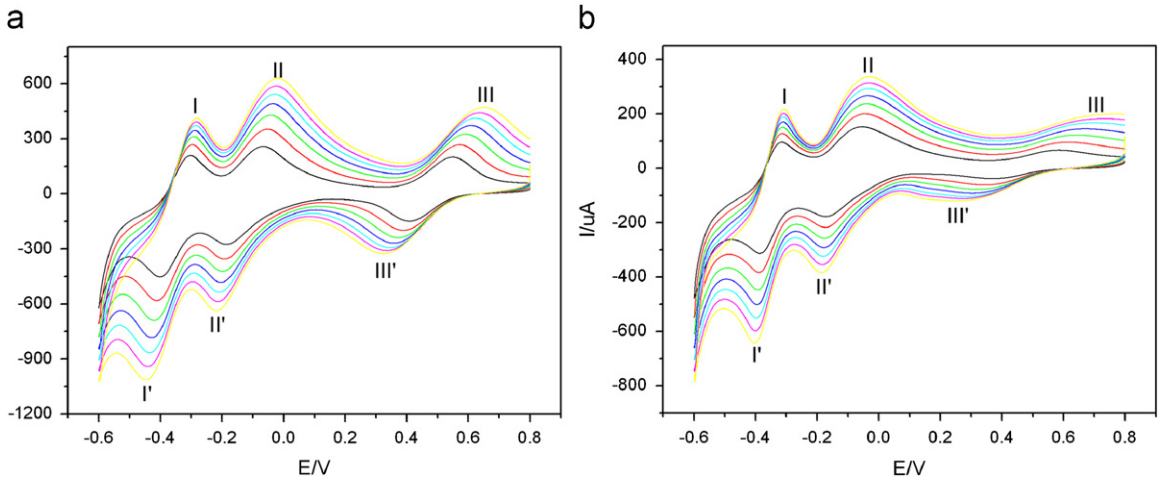

Fig. 7. The cyclic voltammograms of the **1** and **2** CPEs in 1 M H_2SO_4 solution at different scan rates of 50, 80, 110, 140, 170, 200, 230 mV s^{-1}: (a) for **1** and (b) for **2**.

3.5. Magnetic measurements

To check the stability of the network of **1**, the X-ray power diffraction (XRPD) was checked at 20 °C before magnetic study and contrasted to the patterned data curve. As is shown in Fig. S3, the peak positions of simulated and experimental XRPD pattern at 20 °C are in agreement with each other, which indicate the good phase purity of compound **1**. The differences in intensity may be due to the preferred orientation of the crystalline powder samples.

Owning to the same structural comparability that **1** and **2** possess a common $[Mn^{II}O_{14}(H_2O)_2]$ core, the DC magnetic susceptibility (χ_m) of compound **1** was measured in the temperature range 2–300 K with a magnetic field of 1000 Oe for representative. The results ($\chi_m T$ vs. T) are consistent with those of polycrystalline power samples and shown in Fig. 8. When compound **1** is cooled from room temperature to 20 K, the value of $\chi_m T$ increases steadily, this indicates the existence of ferromagnetic interaction between the Mn^{II} ions. The effective magnetic moment calculated from the formula $\mu_{eff}=2.828(\chi_m T)^{1/2}$ at 300 K is 6.16 μ_B, This value is higher than the theoretical one for a spin-only Mn^{II} ions coupling contribution to the moment. The $\chi_m T$ product decreased rapidly at very low temperatures, which might be mainly attributed to the presence of zero-field splitting. The behavior suggests that there exist overall ferromagnetic interactions with the presence of zero-field splitting for Mn^{2+} ions in the compound **1**.

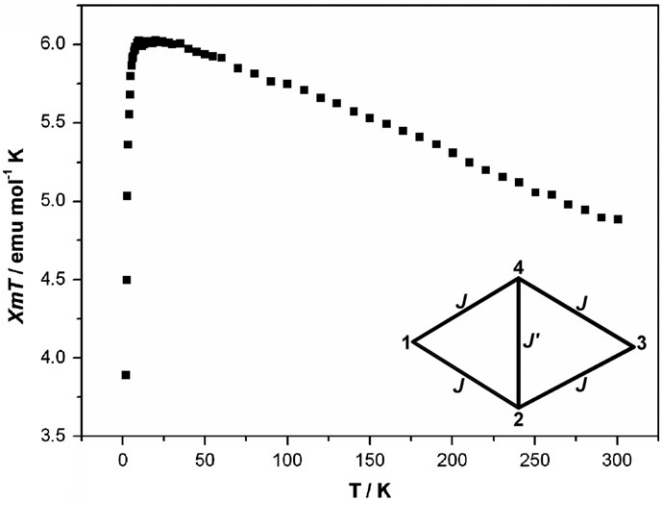

Fig. 8. Temperature dependence of the $\chi_m T$ for **1**.

Between 150 and 300 K, the measured data is consistent with the Curie–Weiss equation, $\chi_m = C/(T-\theta)$, where $C=5.627$ emu K mol^{-1}, $\theta=0.914$ K. This fact further confirms the existence of ferromagnetic interactions between the Mn^{II} $S=5/2$ spins. Indeed, similar magnetic behaviours have been observed in the other polyanions containing the $[Mn^{II}O_{14}(H_2O)_2]$ cluster [13]. The field dependence

of the magnetization below 2 K are shown in Fig. S4. The field dependence of the magnetization below 2 K reveals a rapid increase at low field and tend to reach the saturation state at about 5 T with values of 11.68 μ_B, as expected for system of Mn4 ($S=2$) cores, which confirms the presence of mainly ferromagnetic interactions in compound **1** because magnetization saturation is observed and expect value of magnetization is observed.

4. Conclusions

In this paper, we report the routine synthetic reactions in aqueous solution and crystal structure of two novel high dimensional- and high-connected framework manganese polyoxotungstates which are based on trivacant $[PW_9]$ and $[P_2W_{15}]$ via $Sr(H_2O)_x$ clusters. Compounds **1** and **2** represent $\{4^{20}\cdot 6^{28}\cdot 8^{18}\}\{4^3\}_4$ and $\{4^3\}_2\{4^8\cdot 6^6\cdot 8^{27}\cdot 12^4\}\{4\}_2$ topologies, respectively. It is very rare and interesting that **1** and **2** are 14-modified polyoxotungstates and $Sr(H_2O)_x$ clusters acting as linkages.

Acknowledgments

This work is supported by the National Natural Science Foundation of China (20671026 and 20971032), the Study Technological Innovation Project Special Foundation of Harbin (2009RFXXG202), the Science and Technology Project of Education Office of Heilongjiang Province (11551122), Technological innovation team building program of college of Heilongjiang Province (2009td04) and Innovation Team Research Program of Harbin Normal University (KJTD200902).

Appendix A. Supplementary materials

Supplementary data associated with this article can be found in the online version at doi:10.1016/j.jssc.2010.06.005.

References

[1] (a) M.T. Pope, A. Muller (Eds.), Polyoxometalate Chemistry: From Topology Via Self-Assembly to Applications, Kluwer, Dordrecht, The Netherlands, 2001;
(b) J.J. Borrás-Almenar, E. Coronado, A. Muller, M.T. Pope (Eds.), Polyoxometalate Molecular Science, Kluwer, Dordrecht, The Netherlands, 2004;
(c) M.T. Pope, Comput. Coord. Chem. 4 (2003) 635;
(d) C.L. Hill, Comput. Coord. Chem. 4 (2003) 679.
[2] (a) Y.Y. Yang, L. Xu, G.G. Gao, F.Y. Li, Y.F. Qiu, X.S. Qu, H. Liu, Eur. J. Inorg. Chem. (2007) 2500;
(b) Z.H. Yi, X.B. Cui, X. Zhang, J.Q. Xu, G.D. Yang, Y. Chen, T.G. Wang, X.Y. Yu, J. Mol. Struct. 885 (2008) 149;
(c) B. Keita, I.M. Mbomekalle, L. Nadjo, T.M. Anderson, C.L. Hill, Inorg. Chem. 43 (2004) 257;
(d) H. Liu, C. Qin, Y.G. Wei, L. Xu, G.G. Gao, F.Y. Li, X.S. Qu, Inorg. Chem. 47 (2008) 4166;
(e) W.L. Chen, Y.G. Li, Y.H. Wang, E.B. Wang, Eur. J. Inorg. Chem. (2007) 2216;
(f) R. Khoshnavazi, L. Kaviani, F.M. Zonoz, Inorg. Chim. Acta 362 (2009) 1223;
(g) W.L. Chen, Y.G. Li, Y.H. Wang, E.B. Wang, Z.M. Zhang, Dalton Trans. (2008) 865;
(h) Y. Saku, Y. Sakai, A. Shinohara, K. Hayashi, S. Yoshida, C.N. Kato, K. Yozac, K. Nomiya, Dalton Trans. (2009) 805;
(i) N.L. Laronze, J. Marrot, M. Haouas, F. Taulelle, E. Cadot, Eur. J. Inorg. Chem. (2008) 4920.
[3] (a) C. Craciun, L. David, D. Rusu, M. Rusu, O. Cozar, G.J. Marcu, Radioanal. Nucl. Chem. 247 (2001) 307;
(b) D. Rusu, C. Craciun, A.L. Barra, L. David, M. Rusu, C. Rosu, O. Cozar, G. Marcu, Dalton Trans. (2001) 2879;
(c) D. Rusu, C. Rosu, C. Craciun, L. David, M. Rusu, G. Marcu, J. Mol. Struct. 563 (2001) 427;
(d) P. Mialane, J. Marrot, E. Riviere, J. Nebout, G. Herve, Inorg. Chem. 40 (2001) 44;
(e) U. Kortz, N.K. Al-Kassem, M.G. Savelieff, N.A. AlKadi, M. Sadakane, Inorg. Chem. 40 (2001) 4742;
(f) T.J.R. Weakley, H.T. Evans, J.S. Showell, G.F. Tourne, C.M. Tourne, Chem. Commun. (1973) 139.
[4] (a) P. Mialane, A. Dolbecq, F. Secheresse, Chem. Commun. (2006) 3477;
(b) A. Muller, M.T. Pope, A. Merca, H. Bge, M. Schmidtmann, J.V. Slageren, M. Dressel, D.G. Kurth, Chem. Eur. J. 11 (2005) 5849;
(c) W.L. Chen, Y.G. Li, Y.H. Wang, E.B. Wang, Z.M. Su, Dalton Trans. (2007) 4293.
[5] (a) J.W. Zhao, S.T. Zheng, G.Y. Yang, J. Solid State Chem. 180 (2007) 3317;
(b) J.W. Zhao, B. Li, S.T. Zheng, G.Y. Yang, Cryst. Growth Des. 7 (2007) 2658;
(c) J.W. Zhao, J. Zhang, S.T. Zheng, G.Y. Yang, Chem. Commun. (2008) 570;
(d) S.T. Zheng, J. Zhang, G.Y. Yang, Angew. Chem. Int. Ed. 47 (2008) 3909;
(e) J.W. Zhao, H.P. Jia, J. Zhang, S.T. Zheng, G.Y. Yang, Chem. Eur. J. 13 (2007) 10030;
(f) S.T. Zheng, D.Q. Yuan, J. Zhang, G.Y. Yang, Inorg. Chem. 46 (2007) 4569;
(g) X.K. Fang, C.L. Hill, Angew. Chem. Int. Ed. 46 (2007) 3877;
(h) X.K. Fang, T.M. Anderson, C.L. Hill, Angew. Chem. Int. Ed. 44 (2005) 3540.
[6] (a) S. Chang, Y.F. Qi, E.B. Wang, Z.M. Zhang, Inorg. Chim. Acta 362 (2009) 453;
(b) Z.H. Xu, J. Liu, E.B. Wang, C. Qin, Q. Wu, Q. Shi, J. Mol. Struct. 873 (2008) 41;
(c) Z.M. Zhang, E.B. Wang, Y.G. Li, H.Y. An, Y.F. Qi, L. Xu, J. Mol. Struct. 872 (2008) 176;
(d) Z.M. Zhang, S. Yao, E.B. Wang, C. Qin, C. Qin, J. Solid State Chem. 181 (2008) 715;
(e) W.L. Chen, Y.G. Li, Y.H. Wang, E.B. Wang, Z.M. Su, Dalton Trans. (2007) 4293.
[7] (a) K. Yu, Y.G. Li, B.B. Zhou, Z.H. Su, Z.F. Zhao, Y.N. Zhang, Eur. J. Inorg. Chem. (2007) 5662;
(b) J.P. Wang, K.H. Wang, J.Y. Niu, J. Mol. Struct. 886 (2008) 183.
[8] (a) R. Contant, Inorg. Synth. 27 (1990) 100;
(b) R. Contant, Inorg. Synth. 27 (1990) 108.
[9] (a) G.M. Sheldrick, SHELXS-97, Program for X-ray crystal structure solution, University of Gottingen, Germany, 1997;
(b) G.M. Sheldrick, SHELXL-97, Program for X-ray crystal structure refinement, University of Gottingen, Germany, 1997.
[10] (a) L. Ruhlmann, C.C. Coquelard, J. Canny, R. Thouvenot, Eur. J. Inorg. Chem. (2007) 1493;
(b) C.J. Gómez-García, J.J. Borrás-Almenar, E. Coronado, L. Ouahab, Inorg. Chem. 33 (1994) 4016;
(c) R.G. Finke, T.J.R. Weakley, J. Chem. Crystallogr. 24 (1994) 123.
[11] C.D. Zhang, C.Y. Sun, S.X. Liu, H.M. Ji, Z.M. Su, Inorg. Chim. Acta 363 (2010) 718.
[12] (a) N. Fay, E. Dempsey, T.J. Mccormac, Electroanal. Chem. 574 (2005) 359;
(b) X.G. Cao, L.W. He, B.Z. Lin, Z.J. Chen, P.D. Liu, Inorg. Chim. Acta 362 (2009) 2505.
[13] (a) U. Kortz, S. Nellutla, A.C. Stowe, N.S. Dalal, J. Tol, B.S. Bassil, Inorg. Chem. 43 (2004) 144;
(b) U. Kortz, S. Isber, M.H. Dickman, D. Ravot, Inorg. Chem. 39 (2000) 2915.